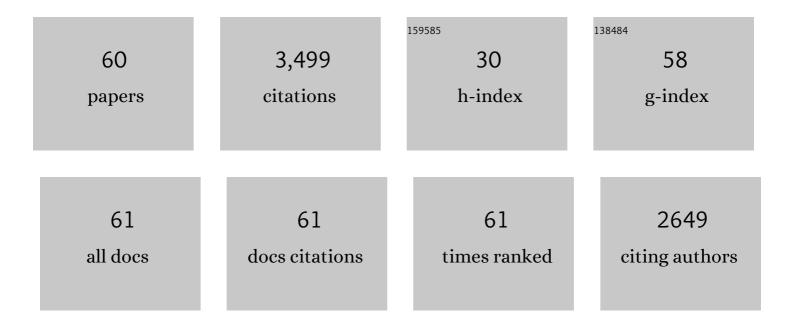
Yujiao Li

List of Publications by Year in descending order

Source: https://exaly.com/author-pdf/3321650/publications.pdf Version: 2024-02-01



ΥμιλοΤι

#	Article	IF	CITATIONS
1	Complexâ€Solidâ€Solution Electrocatalyst Discovery by Computational Prediction and Highâ€Throughput Experimentation**. Angewandte Chemie - International Edition, 2021, 60, 6932-6937.	13.8	86
2	Complexâ€Solidâ€Solution Electrocatalyst Discovery by Computational Prediction and Highâ€Throughput Experimentation**. Angewandte Chemie, 2021, 133, 7008-7013.	2.0	8
3	Effect of cooling rate on the microstructure and mechanical properties of a low-carbon low-alloyed steel. Journal of Materials Science, 2021, 56, 11098-11113.	3.7	6
4	Investigation of an atomicâ€layerâ€deposited Al ₂ O ₃ diffusion barrier between Pt and Si for the use in atomic scale atom probe tomography studies on a combinatorial processing platform. Surface and Interface Analysis, 2021, 53, 727-733.	1.8	1
5	Correlation between grain size and carbon content in white etching areas in bearings. Acta Materialia, 2021, 215, 117048.	7.9	13
6	Atomic scale understanding of phase stability and decomposition of a nanocrystalline CrMnFeCoNi Cantor alloy. Applied Physics Letters, 2021, 119, 201910.	3.3	3
7	Moving cracks form white etching areas during rolling contact fatigue in bearings. Materials Science & Engineering A: Structural Materials: Properties, Microstructure and Processing, 2020, 771, 138659.	5.6	38
8	High temperature creep resistance of a thermally stable nanocrystalline Fe-5 at.% Zr steel. Scripta Materialia, 2020, 179, 1-5.	5.2	28
9	Generalized stability criterion for exploiting optimized mechanical properties by a general correlation between phase transformations and plastic deformations. Acta Materialia, 2020, 201, 167-181.	7.9	34
10	Phase decomposition in a nanocrystalline CrCoNi alloy. Scripta Materialia, 2020, 188, 259-263.	5.2	9
11	Mechanism of collective interstitial ordering in Fe–C alloys. Nature Materials, 2020, 19, 849-854.	27.5	32
12	Revealing the two-step nucleation and growth mechanism of vanadium carbonitrides in microalloyed steels. Scripta Materialia, 2020, 187, 350-354.	5.2	24
13	Solute hydrogen and deuterium observed at the near atomic scale in high-strength steel. Acta Materialia, 2020, 188, 108-120.	7.9	64
14	Photocurrent Recombination Through Surface Segregation in Al–Cr–Fe–O Photocathodes. Zeitschrift Fur Physikalische Chemie, 2020, 234, 605-614.	2.8	3
15	Correlative chemical and structural investigations of accelerated phase evolution in a nanocrystalline high entropy alloy. Scripta Materialia, 2020, 183, 122-126.	5.2	14
16	Direct Observation of Hydrogen in Cold-Drawn Pearlitic Steel Wires Using Cryogenic Atom Probe Tomography. Microscopy and Microanalysis, 2019, 25, 2522-2523.	0.4	1
17	Effect of Nb on improving the impact toughness of Mo-containing low-alloyed steels. Journal of Materials Science, 2019, 54, 7307-7321.	3.7	10
18	Accelerated atomic-scale exploration of phase evolution in compositionally complex materials. Materials Horizons, 2018, 5, 86-92.	12.2	72

Υυίιαο Li

#	Article	IF	CITATIONS
19	On the detection of multiple events in atom probe tomography. Ultramicroscopy, 2018, 189, 54-60.	1.9	59
20	Multiscale Characterization of Microstructure in Near-Surface Regions of a 16MnCr5 Gear Wheel After Cyclic Loading. Jom, 2018, 70, 1758-1764.	1.9	0
21	On the origin of the improvement of shape memory effect by precipitating VC in Fe–Mn–Si-based shape memory alloys. Acta Materialia, 2018, 155, 222-235.	7.9	60
22	Atomic-scale investigation of fast oxidation kinetics of nanocrystalline CrMnFeCoNi thin films. Journal of Alloys and Compounds, 2018, 766, 1080-1085.	5.5	39
23	Grain boundary-constrained reverse austenite transformation in nanostructured Fe alloy: Model and application. Acta Materialia, 2018, 154, 56-70.	7.9	18
24	Influence of microstructure on thermal stability of ultrafine-grained Cu processed by equal channel angular pressing. Journal of Materials Science, 2018, 53, 13173-13185.	3.7	30
25	Multiscale characterization of White Etching Cracks (WEC) in a 100Cr6 bearing from a thrust bearing test rig. Wear, 2017, 370-371, 73-82.	3.1	44
26	Atomic scale characterization of white etching area and its adjacent matrix in a martensitic 100Cr6 bearing steel. Materials Characterization, 2017, 123, 349-353.	4.4	49
27	On the Multiple Event Detection in Atom Probe Tomography. Microscopy and Microanalysis, 2017, 23, 618-619.	0.4	12
28	Deformationâ€Induced Martensite: A New Paradigm for Exceptional Steels. Advanced Materials, 2016, 28, 7753-7757.	21.0	61
29	Ultra-strong and damage tolerant metallic bulk materials: A lesson from nanostructured pearlitic steel wires. Scientific Reports, 2016, 6, 33228.	3.3	49
30	Formation of nanosized grain structure in martensitic 100Cr6 bearing steels upon rolling contact loading studied by atom probe tomography. Materials Science and Technology, 2016, 32, 1100-1105.	1.6	11
31	Defect Recovery in Severely Deformed Ferrite Lamellae During Annealing and Its Impact on the Softening of Cold-Drawn Pearlitic Steel Wires. Metallurgical and Materials Transactions A: Physical Metallurgy and Materials Science, 2016, 47, 726-738.	2.2	20
32	Atomic scale investigation of non-equilibrium segregation of boron in a quenched Mo-free martensitic steel. Ultramicroscopy, 2015, 159, 240-247.	1.9	40
33	Segregation of boron at prior austenite grain boundaries in a quenched martensitic steel studied by atom probe tomography. Scripta Materialia, 2015, 96, 13-16.	5.2	81
34	Mechanisms of subgrain coarsening and its effect on the mechanical properties of carbon-supersaturated nanocrystalline hypereutectoid steel. Acta Materialia, 2015, 84, 110-123.	7.9	60
35	Atomic-Scale Quantification of Grain Boundary Segregation in Nanocrystalline Material. Physical Review Letters, 2014, 112, 126103.	7.8	284
36	Segregation Stabilizes Nanocrystalline Bulk Steel with Near Theoretical Strength. Physical Review Letters, 2014, 113, 106104.	7.8	224

Υυjiao Li

#	Article	IF	CITATIONS
37	Grain boundary segregation engineering in metallic alloys: A pathway to the design of interfaces. Current Opinion in Solid State and Materials Science, 2014, 18, 253-261.	11.5	466
38	Atomic scale investigation of redistribution of alloying elements in pearlitic steel wires upon cold-drawing and annealing. Ultramicroscopy, 2013, 132, 233-238.	1.9	27
39	Influence of supersaturated carbon on the diffusion of Ni in ferrite determined by atom probe tomography. Scripta Materialia, 2013, 69, 424-427.	5.2	16
40	Nanocrystalline Fe–C alloys produced by ball milling of iron and graphite. Acta Materialia, 2013, 61, 3172-3185.	7.9	70
41	Evolution of strength and microstructure during annealing of heavily cold-drawn 6.3 GPa hypereutectoid pearlitic steel wire. Acta Materialia, 2012, 60, 4005-4016.	7.9	187
42	Deformation resistance in the transition from coarse-grained to ultrafine-grained Cu by severe plastic deformation up to 24 passes of ECAP. Materials Science & Engineering A: Structural Materials: Properties, Microstructure and Processing, 2011, 528, 8621-8627.	5.6	41
43	Atomic-scale mechanisms of deformation-induced cementite decomposition in pearlite. Acta Materialia, 2011, 59, 3965-3977.	7.9	269
44	Atom probe tomography characterization of heavily cold drawn pearlitic steel wire. Ultramicroscopy, 2011, 111, 628-632.	1.9	65
45	Metallic composites processed via extreme deformation: Toward the limits of strength in bulk materials. MRS Bulletin, 2010, 35, 982-991.	3.5	180
46	Stability of ultrafine-grained Cu to subgrain coarsening and recrystallization in annealing and deformation at elevated temperatures. Acta Materialia, 2009, 57, 5207-5217.	7.9	55
47	On the elevated-temperature deformation behavior of polycrystalline Cu subjected to predeformation by multiple compression. Materials Science & Engineering A: Structural Materials: Properties, Microstructure and Processing, 2008, 483-484, 547-550.	5.6	1
48	Structural stability of ultrafine-grained copper. Scripta Materialia, 2008, 58, 53-56.	5.2	15
49	Deformation kinetics of nanocrystalline nickel. Acta Materialia, 2007, 55, 5708-5717.	7.9	75
50	Deformation kinetics of coarse-grained and ultrafine-grained commercially pure Ti. Materials Science & Engineering A: Structural Materials: Properties, Microstructure and Processing, 2007, 462, 275-278.	5.6	20
51	Flow stress and creep rate of nanocrystalline Ni. Scripta Materialia, 2007, 57, 429-431.	5.2	25
52	Creep transients during stress changes in ultrafine-grained copper. Scripta Materialia, 2006, 54, 1803-1807.	5.2	23
53	On the Hall–Petch relation between flow stress and grain size. International Journal of Materials Research, 2006, 97, 1661-1666.	0.3	16
54	Deformation kinetics of ultrafine-grained Cu and Ti. Materials Science & Engineering A: Structural Materials: Properties, Microstructure and Processing, 2005, 410-411, 451-456.	5.6	34

Υυjiao Li

#	Article	IF	CITATIONS
55	Creep deformation mechanisms in high-pressure die-cast magnesium-aluminum-base alloys. Metallurgical and Materials Transactions A: Physical Metallurgy and Materials Science, 2005, 36, 1721-1728.	2.2	71
56	Strain rate sensitivity of Cu after severe plastic deformation by multiple compression. Physica Status Solidi (A) Applications and Materials Science, 2005, 202, R119-R121.	1.8	25
57	Influence of grain boundaries on steady-state deformation resistance of ultrafine-grained Cu. Physica Status Solidi A, 2004, 201, 2915-2921.	1.7	14
58	On Coble creep in ultrafine-grained Cu. Physica Status Solidi A, 2004, 201, R114-R117.	1.7	14
59	Does nanocrystalline Cu deform by Coble creep near room temperature?. Materials Science & Engineering A: Structural Materials: Properties, Microstructure and Processing, 2004, 387-389, 585-589.	5.6	38
60	Transition from strengthening to softening by grain boundaries in ultrafine-grained Cu. Acta Materialia, 2004, 52, 5009-5018.	7.9	161